
Resolution of Apoptosis in Atherosclerotic Plaque by Dietary Modification and Statin Therapy

Dagmar Hartung, MD^{1,2}; Masayoshi Sarai, MD²; Artiom Petrov, PhD²; Frank Kolodgie, PhD³; Navneet Narula, MD²; Johan Verjans, MD²; Renu Virmani, MD³; Chris Reutelingsperger, PhD⁴; Leo Hofstra, MD, PhD⁴; and Jagat Narula, MD, PhD²

¹School of Medicine Hannover, Hannover, Germany; ²Division of Cardiology, University of California, Irvine, Irvine, California; ³Cardiovascular Pathology, Gaithersburg, Maryland; and ⁴University Hospital Maastricht, Maastricht, The Netherlands

Although apoptosis within atherosclerotic plaques is associated with plaque vulnerability and rupture, the role of inhibition of the apoptotic process is not clear. We evaluated the impact of dietary modification and statin therapy (measures known to favorably influence outcomes in coronary disease) on the incidence of apoptosis in experimental atherosclerotic lesions. **Methods:** A total of 30 animals were studied; 1 group of 6 animals served as the controls (group 1), and the remaining 24 animals were subjected to balloon de-endothelialization of the abdominal aorta and a high-cholesterol diet. These atherosclerotic animals were randomized as follows: high-cholesterol diet for 4 mo ($n = 6$; untreated atherosclerotic group [group 2]), high-cholesterol diet for 3 mo and normal chow diet for 1 mo ($n = 6$; diet withdrawal group [group 3]), and high-cholesterol diet for 4 mo and simvastatin orally every day of the last month ($n = 6$; statin therapy group [group 4]). ^{99m}Tc-Annexin A5 was used for noninvasive detection of apoptosis in groups 1–4. The remaining 6 rabbits on a high-cholesterol diet for 4 mo were studied with radio-labeled mutant annexin A5 ($n = 6$; nonspecific control group [group 5]). Quantitative annexin A5 uptake in the abdominal aorta was determined and compared with the histologic and immunohistochemical characteristics of the atherosclerotic lesions. **Results:** Maximum annexin A5 uptake (mean \pm SD, 0.051 ± 0.009 percentage injected dose per gram [%ID/g] of tissue) was observed in the untreated atherosclerotic animals. The uptake was substantially reduced in the diet withdrawal (0.03 ± 0.006 %ID/g; $P < 0.0001$) and statin therapy (0.03 ± 0.006 %ID/g; $P < 0.0001$) groups. The plaques in the untreated high-cholesterol group demonstrated advanced atherosclerotic lesions. On the other hand, the diet withdrawal and statin therapy groups showed histologic characteristics of stabilization, including the resolution of macrophage infiltration and an increase in smooth muscle cell content. There was a marked reduction in the apoptosis of macrophages. No significant uptake of annexin A5 or mutant annexin A5 was seen in rabbits on the normal chow diet or

atherosclerotic rabbits, respectively. **Conclusion:** Dietary modification and statin therapy in atherosclerosis lead to a reduction in apoptosis and contribute to plaque stabilization. It can be hypothesized that a reduction in apoptosis is a favorable process in atherosclerotic disease.

Key Words: programmed cell death; atheroma; 3-hydroxy-3-methylglutaryl coenzyme A reductase inhibitors

J Nucl Med 2005; 46:2051–2056

In up to two thirds of patients, acute coronary events result from the rupture of atherosclerotic plaque (1). The plaque vulnerable to rupture is characterized by distinct histologic characteristics, including large lipid cores, attenuated fibrous caps less than 65 μ m thick, and intense inflammation of the fibrous caps (2). Extensive apoptosis of inflammatory cells is observed in the fibrous cap associated with rupture of the plaque (3,4). Whereas the reduction in total plaque lipid burden, resolution of inflammation, and neutralization of matrix metalloproteinase expression are known to contribute to plaque stabilization (5), the role of prevention of apoptosis is not clear. Because apoptosis has been shown to be related to plaque instability and because dietary modification and statin therapy are related to the prevention of acute coronary syndrome, we evaluated the role of these interventions in the prevalence of apoptosis in experimental atherosclerotic lesions.

For the noninvasive evaluation of apoptosis in atherosclerotic lesions, we used annexin A5 labeled with ^{99m}Tc for radionuclide imaging. Annexin A5, a naturally occurring protein, has a nanomolar affinity for binding to phosphatidylserine (PS), which is prominently expressed on the outer cell membrane surface of apoptotic cells (6,7). ^{99m}Tc-labeled annexin A5 has been successfully used for the noninvasive imaging of apoptosis in atherosclerotic plaques in various experimental atherosclerosis models and for the detection of apoptosis in carotid artery atherosclerotic disease in patients undergoing carotid endarterectomy (8–10).

Received Jul. 1, 2005; revision accepted Sep. 6, 2005.
For correspondence or reprints contact: Artiom Petrov, PhD, Division of Cardiology, University of California, Irvine, Medical Sciences I, Room C116, Irvine, CA 92697.
E-mail: adpetrov@uci.edu

MATERIALS AND METHODS

Experimental Model of Atherosclerosis

Atherosclerosis was induced in male New Zealand White rabbits (2.5–3.5 kg; Millbrook Breeding Laboratories) by de-endothelialization of the infradiaphragmatic aorta with a 4F Fogarty embolectomy catheter (12-040-4F; Edwards Lifesciences LLC) as described previously (8). Briefly, the right femoral artery was surgically exposed under general anesthesia (ketamine–xylazine, 100 mg/mL, 10:1 [v/v]; 1.5–2.5 mL subcutaneously). A small arteriotomy site was created, and the embolectomy catheter was advanced in the aorta up to the level of the diaphragm. After inflation to a pressure of 3 psi, the catheter was pulled 3 times antegrade to the bifurcation of the aorta and removed. The femoral artery was ligated, and the incision site was closed. A high-cholesterol diet (0.5% cholesterol and 6% peanut oil) was started 1 wk before surgery and continued for an additional 15 wk for the induction of atherosclerotic lesions. The study conformed to the *Guide for the Care and Use of Laboratory Animals* (11), and the Institutional Laboratory Animal Care and Use Committee approved the study protocol.

Study Protocol

A total of 30 New Zealand White rabbits were included in the study. Group 1 consisted of 6 rabbits that did not undergo balloon de-endothelialization and were fed a normal chow diet for 16 wk. Group 1 animals comprised the control group. Group 2 rabbits had balloon de-endothelialization of the infradiaphragmatic aorta and were fed the high-cholesterol diet for 4 mo ($n = 6$, untreated atherosclerotic group). Group 3 rabbits had balloon de-endothelialization and were fed the high-cholesterol diet for 3 mo followed by a normal chow diet for 1 mo ($n = 6$, diet withdrawal group). Group 4 rabbits had balloon de-endothelialization and were fed the high-cholesterol diet for 4 mo; in the final month of the experiment, these animals were treated with simvastatin (3-hydroxy-3-methylglutaryl coenzyme A reductase inhibitor; Merck) at 1 mg/kg/d orally ($n = 6$, statin therapy group). For molecular imaging and quantitative assessment of apoptosis in atherosclerotic plaques of groups 1–4, annexin A5 labeled with ^{99m}Tc was administered intravenously. Group 5 rabbits underwent balloon de-endothelialization and were fed the high-cholesterol diet for 4 mo ($n = 6$), like untreated atherosclerotic group 2; however, group 5 animals were imaged instead with a mutant form of annexin A5 that does not bind to PS (Table 1). Group 5 animals served as the nonspecific control group.

Serial blood samples were drawn for blood clearance at 0, 1, 2, and 3 h after radiotracer administration. Left lateral decubitus

images were obtained as described below. After imaging, animals were sacrificed with an overdose of sodium pentobarbital (120 mg/kg). Aortas were carefully removed, and ex vivo γ -images of the excised aortas were obtained. The aorta was segmented at 1-cm intervals, each segment was weighed, and activity in each specimen was counted in an automatic γ -well-type scintillation counter (Perkin-Elmer–Wallac Inc.). The activity in each specimen was compared with the activity in an aliquot of the injected dose to express the uptake in the aortic segment as the percentage injected dose per gram (%ID/g) of tissue. Aortas from 2 animals in each group were preserved for histologic and immunohistochemical investigation as explained below.

Radionuclide Labeling and Imaging Procedure

Human recombinant annexin A5, expressed in *Escherichia coli*, was derivatized with nicotinic acid analog hydrazinonicotinamide (HYNIC; Theseus Imaging Corp.) as described previously (12). To bind ^{99m}Tc to the HYNIC–annexin A5 conjugate, a reduced tin (stannous ion) and Tricine (*N*-tris[hydroxymethyl]methylglycine; Sigma-Aldrich) solution was added to ^{99m}Tc -pertechnetate with an aliquot of HYNIC–annexin A5 under anoxic conditions. Thin-layer chromatography showed a radiopurity of about 95%–98%. Animals were injected intravenously with 0.5–1 mg of annexin A5 labeled with approximately 200 ± 60 MBq of ^{99m}Tc (mean \pm SD). However, in group 5 animals, M1234, a mutant form of annexin A5, was administered. M1234 lacks binding to PS and to apoptotic cells in the presence of physiologic calcium concentrations. The mutant annexin A5 has defective calcium binding sites in its 4 domains because of replacements of the critical amino acids E72, D144, E228, and D303 with the amino acids Q, N, A, and N, respectively. The mutant was constructed by site-directed mutagenesis of the complementary DNA of annexin A5, expressed in *E. coli*, and purified as described previously (13).

Images in the left lateral decubitus position were obtained immediately and at 1, 2, and 3 h after radionuclide administration by use of a γ -camera (Vertex PLUS; ADAC) equipped with a low-energy, high-resolution, parallel-hole collimator. The images were acquired centered on a 140-keV photopeak of ^{99m}Tc with a symmetric 20% window and a 128×128 word matrix. Planar images of whole rabbits were obtained for 15 min. The isolated aorta was imaged for 30 min. Total serum cholesterol in representative animals was measured colorimetrically by use of a cholesterol oxidase enzymatic kit (Infinity Cholesterol; Sigma Diagnostics, Inc.).

Histologic and Immunohistochemical Characterization of Atherosclerotic Lesions

We processed representative aortic tissue specimens for histopathologic and immunohistochemical studies; histologic specimens were collected from 2 animals in each group. In situ end labeling also was performed for the assessment of apoptosis. However, for the present study, we relied entirely on annexin A5 uptake as an index of the severity of the apoptotic process. As described previously (8), one half of every aortic segment was snap frozen. The other half was fixed with *N*-(2-hydroxyethyl) piperazine-*N'*-(2-ethansulfonic acid)-buffered formalin (4%) and Ca^{2+} (2 mmol/L), dehydrated, and embedded in paraffin. Serial 4- μm -thick cross sections were cut and mounted on charged slides (Superfrost; Fisher). Tissue sections were stained with Movat pentachrome elastin stain and with hematoxylin and eosin. Histologic specimens were analyzed on the basis of the classification scheme of the American Heart Association (AHA) (14). AHA type II lesions contain few layers of macrophage-derived intimal foam

TABLE 1
Classification of Study Groups

Group ($n = 6$)	Duration of diet (mo)		Intervention	Imaging agent
	High cholesterol	Normal chow		
1		4		Annexin A5
2	4			Annexin A5
3	3	1		Annexin A5
4	4		Simvastatin in mo 4	Annexin A5
5	4			Mutant annexin A5

cells, smooth muscle cells (SMC), and extracellular matrix; type III lesions show focal acellular areas containing extracellular lipid pools and are rich in proteoglycans; and type IV lesions have a necrotic core, calcification within the deep intimal layers, and a fibrous cap. More advanced lesion types are not observed in a rabbit model of de-endothelialization and high-cholesterol diet. After tissue sections were deparaffinized in xylene and treated with 0.3% hydrogen peroxide for 20 min, they were incubated in protein-free block (Dako) for 10 min to inhibit the nonspecific binding of primary antibody. SMC were localized with a primary antibody against actin isotypes α and β (HHF-35 [Enzo]; 1:40 dilution; 1 h of incubation), and macrophages were identified with RAM-11 (Dako; 1:200 dilution; overnight incubation). As described previously (8), primary antibodies were labeled with a biotinylated link antibody directed against mice by use of a peroxidase-based kit (LSAB; Dako), and immunostains were visualized by use of an AEC substrate-chromogen system (Dako) and then counterstained with Gill hematoxylin. In addition, DNA fragmentation was detected for the localization of apoptosis in atherosclerotic lesions. For this purpose, terminal deoxynucleotidyltransferase-mediated deoxyuridine triphosphate nick-end labeling was used in accordance with the instructions in an in situ apoptosis detection kit (TACS; Trevigen).

Statistical Analysis

The γ -scintillation counts were calculated as %ID/g of tissue or blood. Results are expressed as mean \pm SD. To determine the statistical significance of differences between groups, 1-tailed ANOVA followed by the Fisher post hoc test for multiple comparisons was used. Differences were considered to be significant at $P < 0.05$.

RESULTS

Noninvasive Imaging of Abdominal Atherosclerotic Lesions

The γ -imaging allowed noninvasive visualization of atherosclerotic lesions in the abdominal aorta; the most visible lesions were the abdominal lesions in group 2 untreated

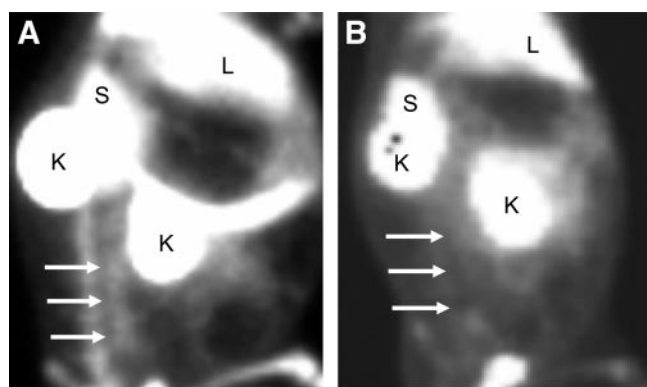


FIGURE 1. Noninvasive imaging of apoptosis with radiolabeled annexin A5. Left lateral oblique γ -images of experimental atherosclerotic rabbit (A) and control rabbit (B) at 3 h after injection of ^{99m}Tc -annexin A5 are shown. Uptake of annexin A5 is clearly seen in abdominal atherosclerotic lesions (A; arrows). In contrast, uptake of radiotracer is absent in abdominal aorta of control rabbit (B; arrows). L = liver activity; K = kidney activity; S = splenic activity.

atherosclerotic rabbits (Fig. 1). The results were confirmed in ex vivo images of explanted aortas (Fig. 2A). No annexin A5 uptake was observed in group 1 control rabbits, which had received normal chow for 4 mo, or in group 5 atherosclerotic rabbits, for which mutant annexin A5 was used for nuclear imaging (nonspecific control). Only negligible annexin A5 uptake was observed in the diet withdrawal (group 3) and statin therapy (group 4) groups. The total serum cholesterol level in group 1 animals was 1.6 ± 0.8 mmol/L, and this level was increased significantly in group 2 animals (44.1 ± 9.8 mmol/L) ($P < 0.001$). Diet withdrawal resulted in a significant reduction in the cholesterol level (18.6 ± 9.5 mmol/L) ($P = 0.001$); the cholesterol level was statistically insignificantly lower in the statin therapy group (37.5 ± 10.3 mmol/L) (P was not significant).

Quantitative ^{99m}Tc -Annexin A5 Uptake

The calculated %ID/g for the uptake of annexin A5 in aortic lesions was significantly higher in group 2 untreated atherosclerotic animals (0.051 ± 0.009 ; $P = 0.0001$) than in other groups (Fig. 2B). The annexin A5 uptake was confined to the atherosclerotic regions. The uptake was reduced significantly in group 3, for which the diet was replaced with a normal chow diet in the fourth month (0.03 ± 0.006 %ID/g; absolute reduction of 42%; $P = 0.0001$), or in the statin therapy group (group 4), for which the high-cholesterol diet was supplemented with simvastatin for 1 mo (0.03 ± 0.006 %ID/g; absolute reduction of 41%; $P = 0.0001$). Annexin A5 uptake was reduced significantly in the latter group, although the cholesterol level was not reduced as much as in the diet withdrawal group.

Histologic and Immunohistochemical Characteristics of Atherosclerotic Lesions

As reported earlier (8), specific annexin A5 uptake preferentially occurs in advanced AHA type IV atherosclerotic plaques; the uptake was traced to apoptotic macrophages by dual immunohistochemical staining techniques. In the present study, the lesions in the group 2 animals (high-cholesterol diet) were extensive; these lesions were predominantly macrophage rich, with minimal SMC content, and showed extensive apoptosis (Fig. 3). A comparison of histologic and scintigraphic data showed that uptake occurred predominantly in AHA type IV lesions, which harbored significant apoptosis of macrophages. The diet withdrawal and statin therapy groups showed decreases in macrophage populations and increases in SMC content (Fig. 4). In addition, there was a marked decrease in apoptosis.

DISCUSSION

Apoptosis occurs commonly in advanced atherosclerotic plaques and potentially contributes to plaque vulnerability and rupture (15). Morphologic data suggest that apoptosis of macrophages adds to enlargement of the lipid core (15). In addition, extensive apoptosis of macrophages occurs at sites of plaque rupture and likely initiates events leading to

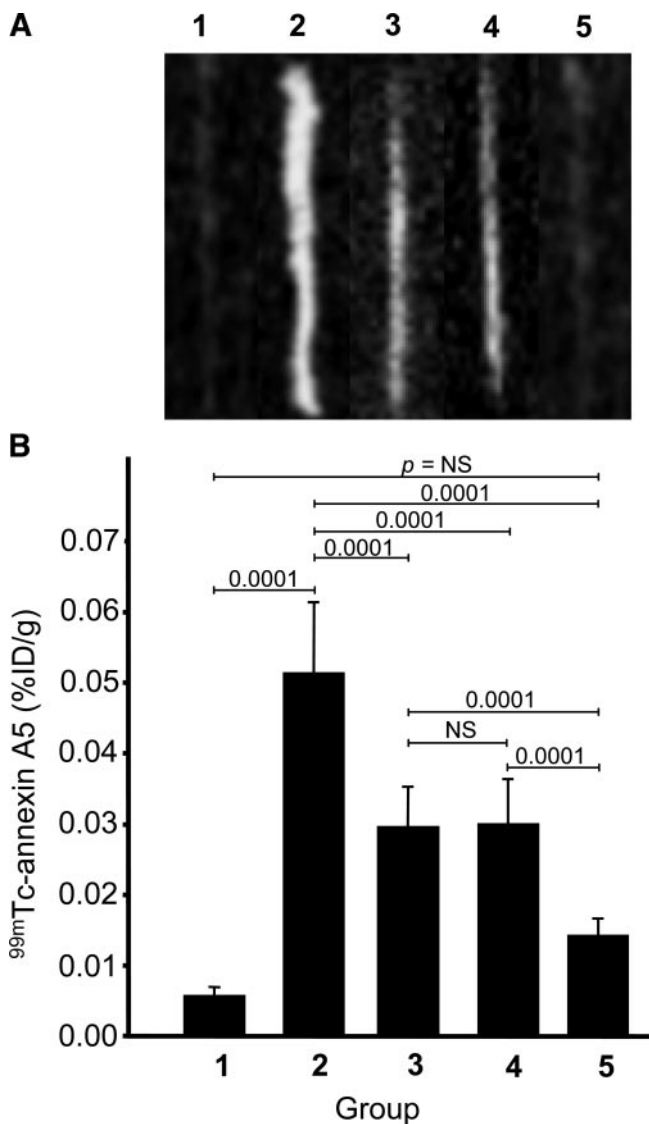


FIGURE 2. ^{99m}Tc -Annexin A5 uptake within abdominal aortas in various study groups. (A) Ex vivo images of explanted aortas (groups 1–5) show intense annexin A5 uptake within abdominal aortas in rabbits fed high-cholesterol diet for 4 mo (group 2); only negligible annexin A5 uptake was seen in diet withdrawal (group 3) and statin therapy (group 4) groups. No annexin A5 uptake was observed in control rabbits receiving normal chow diet for 4 mo (group 1) or in rabbits receiving high-cholesterol diet for 4 mo and imaged with mutant annexin A5 (group 5). (B) Bar graphs show quantitative ^{99m}Tc -annexin A5 uptake within abdominal aortas in various study groups, represented as mean \pm SD %ID/g; annexin A5 uptake corresponds to ex vivo images in A. Maximum ^{99m}Tc -annexin A5 uptake (%ID/g) was seen in group 2 animals ($P = 0.0001$) compared with group 1 animals (controls). Uptake was significantly lower in diet withdrawal and statin therapy groups than in group 2 animals. No significant difference was observed between animals in diet withdrawal group and animals in statin therapy group or between animals in group 1 (controls) and animals imaged with mutant annexin A5 (group 5) (P was not significant [NS]). Quantitative results confirmed ex vivo imaging observations.

rupture (4). Annexin A5 was recently used for the noninvasive localization of apoptosis in atherosclerotic plaques (8). The uptake was correlated directly with the prevalence of apoptosis and the extent of macrophage infiltration. Annexin A5 uptake did not show any relationship with the SMC content of lesions. Maximum uptake, like apoptosis, was seen in advanced AHA type IV atherosclerotic lesions. Apoptosis was seen almost exclusively in macrophages. In the present investigation as well, there was significant uptake of annexin A5 in animals with atherosclerotic lesions, but mutant annexin A5 uptake was not observed in similarly produced lesions, confirming the specificity of the noninvasive imaging strategy. Similarly, there was no uptake of annexin A5 in normal aortas from control rabbits as well as unaffected aortic regions in atherosclerotic rabbits.

The extent of apoptosis was markedly decreased in the diet withdrawal and statin therapy groups, with histopathologic evidence of stabilization of plaques, as represented by decreased macrophage infiltration and increased SMC content. Whereas the stabilization of the plaque is understandable with a decrease in the cholesterol level in the diet withdrawal group, the stabilization in the statin group with a relatively small change in the cholesterol level is intriguing. The small change in the cholesterol level in the statin therapy group was attributable to the continuation of a high-cholesterol diet. Stabilization of plaques, reduction in apoptosis, and lower annexin A5 uptake may be ascribed to pleiotropic effects of statins that are independent of the cholesterol level (16–18). Pleiotropic effects may include a decrease in inflammation and oxidative stress in atherosclerotic plaques. Statins inhibit the formation of mevalonic acid and downstream isoprenoid products (such as geranylgeranylpyrophosphate) that lead to the downregulation of myeloperoxidase gene expression in macrophages. Myeloperoxidase promotes the oxidation of lipoproteins (19). The isoprenoid intermediates are used by lipids to attach to several intracellular signaling molecules to control the activity of signaling pathways.

The present study demonstrates that a decrease in apoptosis was associated with behavioral and therapeutic interventions known to improve outcomes in coronary artery disease. If a reduction in apoptosis is considered to be a favorable event, it will become possible to develop strategies to therapeutically target the apoptotic process. After an acute coronary event, recurrences occur most commonly within the next 4 wk, with a gradual decrease by 3 mo (20) and 1 y (21). A significant decrease in the incidence of recurrences has been demonstrated at 4 mo–1 y after the index acute coronary event with the help of statin therapy. Even with immediate postinfarction use of aggressive doses of atorvastatin, the outcome curves do not separate at least until 4 wk (20). It is logical to assume that treatment with statins, through cholesterol-lowering and pleiotropic effects, may take up to 4 wk to demonstrate the beneficial effect of plaque stabilization. Given that apoptosis contributes to

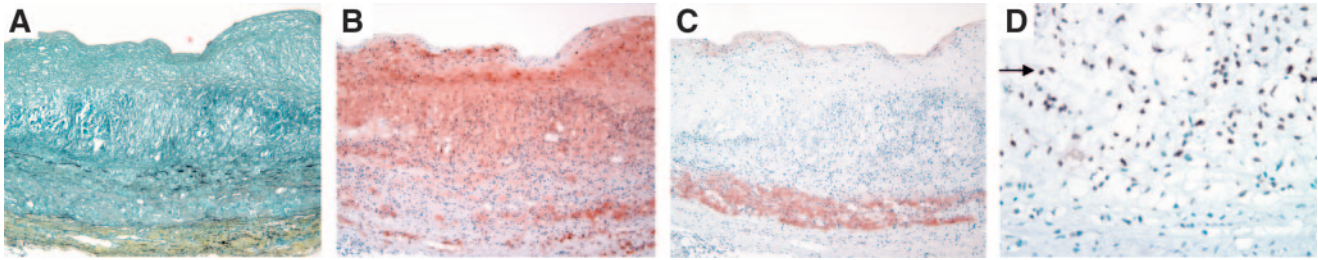


FIGURE 3. Histologic and immunohistochemical characteristics of atherosclerotic lesions. Photomicrographs of abdominal atherosclerotic lesions from untreated atherosclerotic animal of group 2 are shown. (A) Movat pentachrome stain ($\times 100$) demonstrates AHA type IV lesion with well-formed necrotic core in neointimal region. (B) Staining with antibody specific for macrophages (CD68; RAM-11) ($\times 100$) shows widespread presence of macrophage infiltration in neointima. (C) Staining with antibody against actin isotypes α and β (HHF-35) to identify SMC ($\times 100$) shows absence of SMC in neointima. SMC staining is visible only in normal medial layer of atherosclerotic vessel. (D) DNA fragmentation staining (blue–black nuclei; arrow) by in situ end labeling and methyl green counterstaining (blue–green nuclei) ($\times 200$) demonstrate extensive apoptosis of macrophages.

plaque vulnerability, manipulation of apoptosis in atherosclerotic plaques may be of clinical value. It may be worthwhile to evaluate the beneficial effects of caspase inhibitors for containing apoptosis. Such a strategy may have amplified impact because caspase inhibitors significantly delay direct myocardial damage associated with ischemic insult (22).

CONCLUSION

This assessment confirmed that a decrease in the apoptosis of inflammatory cells occurs in parallel with favorable

alterations in atherosclerotic plaques. In other words, the prevention of apoptosis also should fall within the spectrum of plaque stabilization and should be considered a favorable histologic change. This study confirms the feasibility of the use of annexin A5 for imaging of atherosclerotic lesions and for serial imaging to demonstrate interval changes in the incidence of apoptosis with therapeutic interventions. This study also demonstrates that statin therapy may result in plaque alterations disproportionately greater than expected from a decrease in serum cholesterol content.

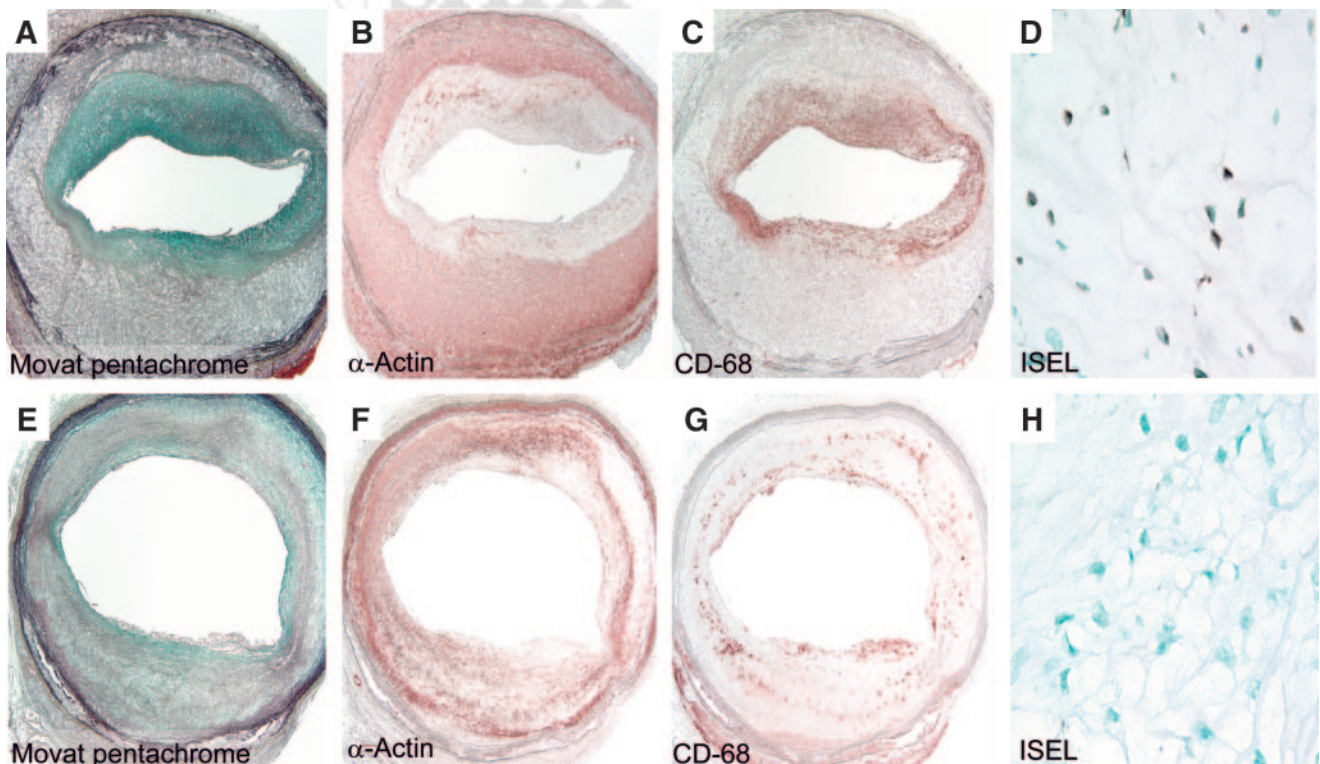


FIGURE 4. Stabilization of atherosclerotic lesions in diet withdrawal and statin therapy groups. Increased SMC content, decreased macrophage populations, and decreased apoptosis were observed after diet withdrawal (A–D) and statin therapy (E–H). Micrographs of cross sections of abdominal aortas stained with Movat pentachrome (A and E), HHF-35 (B and F), and RAM-11 (C and G) ($\times 30$) and micrographs after DNA fragmentation staining by in situ end labeling (ISEL) ($\times 200$) (D and H) are shown. Decreased macrophage populations (C and G), increased SMC content (B and F), and decreased apoptosis (D and H) represent histologic evidence of stabilization of plaques.

ACKNOWLEDGMENT

This study was supported by National Institutes of Health grant 1 RO1 HL68657-01.

REFERENCES

1. Burke A, Farb A, Malcolm GT, Liang YH, Smialek J, Virmani R. Coronary risk factors and plaque morphology in men with coronary artery disease who died suddenly. *N Engl J Med.* 1997;336:1276–1282.
2. Virmani R, Kolodgie FD, Burke AP, Farb A, Schwartz SM. Lessons from sudden coronary death: a comprehensive morphological classification scheme for atherosclerotic lesions. *Arterioscler Thromb Vasc Biol.* 2000;20:1262–1275.
3. Galis ZS, Sukhova GK, Lark MW, Libby P. Increased expression of matrix metalloproteinases and matrix degrading activities in vulnerable regions of human atherosclerotic plaques. *J Clin Invest.* 1994;94:2493–2503.
4. Kolodgie F, Narula J, Burke AP, et al. Localization of apoptotic macrophages at the site of plaque rupture in sudden coronary death. *Am J Pathol.* 2000;157:1259–1268.
5. Libby P, Ridker PM, Maseri A. Inflammation and atherosclerosis. *Circulation.* 2002;105:1135–1143.
6. Dachary-Prigent J, Freyssinet JM, Pasquet JM, Carron JC, Nurden AT. Annexin V as a probe of aminophospholipid exposure and platelet membrane vesiculation: a flow cytometry study showing a role for free sulfhydryl groups. *Blood.* 1993;81:2554–2565.
7. Fadok VA, Voelker DR, Campbell PA, Cohen JJ, Bratton DL, Henson PM. Exposure of phosphatidylserine on the surface of apoptotic lymphocytes triggers specific recognition and removal by macrophages. *J Immunol.* 1992;148:2207–2216.
8. Kolodgie FD, Petrov A, Virmani R, et al. Targeting of apoptotic macrophages and experimental atheroma with radiolabeled annexin V: a technique with potential for noninvasive imaging of vulnerable plaque. *Circulation.* 2003;108:3134–3139.
9. Johnson LL, Narula N, Schonfield L, Chaves L, Narula J. Tc-99m-Annexin-V imaging for detection of atherosclerotic lesions in porcine coronary artery [abstract]. *J Am Coll Cardiol.* 2003;41(suppl A):445A.
10. Kietsealer BL, Reutelingsperger CP, Heidendal GA, et al. Noninvasive detection of plaque instability with use of radiolabeled annexin A5 in patients with carotid artery atherosclerosis. *N Engl J Med.* 2004;350:1472–1473.
11. *Guide for the Care and Use of Laboratory Animals.* Washington, DC: National Academy Press; 1996.
12. Blankenberg FG, Katsikis PD, Tait JF, et al. In vivo detection and imaging of phosphatidylserine expression during programmed cell death. *Proc Natl Acad Sci USA.* 1998;95:6349–6354.
13. Kenis H, van Genderen H, Benhaghmouch A, et al. Cell surface-expressed phosphatidylserine and annexin A5 open a novel portal of cell entry. *J Biol Chem.* 2004;279:52623–52629.
14. Sary HC, Chandler AB, Dinsmore RE, et al. A definition of initial, fatty streak, and intermediate lesions of atherosclerosis: a report from the Committee on Vascular Lesions of the Council on Atherosclerosis, American Heart Association. *Arterioscler Thromb Vasc Biol.* 1994;14:840–856.
15. Bjorkerud S, Bjorkerud B. Apoptosis is abundant in human atherosclerotic lesions, especially in inflammatory cells (macrophages and T cells), and may contribute to the accumulation of gruel and plaque instability. *Am J Pathol.* 1996;149:367–380.
16. Hansson KG. Inflammation, atherosclerosis, and coronary artery disease. *N Engl J Med.* 2005;352:1685–1695.
17. Kumar AP, Reynolds WF. Statins downregulate myeloperoxidase gene expression in macrophages. *Biochem Biophys Res Commun.* 2005;331:442–451.
18. Takemoto M, Liao JK. Pleiotropic effects of 3-hydroxy-3-methylglutaryl coenzyme A reductase inhibitors. *Arterioscler Thromb Vasc Biol.* 2001;21:1712–1719.
19. Nicholls SJ, Hazen SL. Myeloperoxidase and cardiovascular disease. *Arterioscler Thromb Vasc Biol.* 2005;25:1102–1111.
20. Schwartz GG, Olsson AG, Ezekowitz MD, et al. Effects of atorvastatin on early recurrent ischemic events in acute coronary syndromes: the MIRACL study—a randomized controlled trial. *JAMA.* 2001;285:1711–1718.
21. Kjekshus J, Pedersen TR. Reducing the risk of coronary events: evidence from the Scandinavian Simvastatin Survival Study (4S). *Am J Cardiol.* 1995;76:64C–68C.
22. Dumont EA, Reutelingsperger CP, Smits JF, et al. Real-time imaging of apoptotic cell-membrane changes at the single-cell level in the beating murine heart. *Nat Med.* 2001;7:1352–1355.